Subcellular Localization of Cerebellar Degeneration-Related Protein 1

Eirik Tveit Solheim
Haukeland Universitetssjukehus https://orcid.org/0000-0001-9318-8388
Torbjørn Kråkenes
Universitetet i Bergen Det medisinsk-odontologiske fakultet
Cecilie Totland
Helse Bergen HF
Christian Alexander Vedeler (christian.alexander.vedeler@helse-bergen.no)
Universitetet i Bergen Det medisinsk-odontologiske fakultet

Research article

Keywords: Paraneoplastic cerebellar degeneration, neurodegeneration, cancer, CDR1, mitochondria, cytoskeleton, STED microscopy

Posted Date: July 1st, 2020

DOI: https://doi.org/10.21203/rs.3.rs-36876/v1

Abstract

Background: Cerebellar degeneration-related protein 1 (CDR1) is associated with paraneoplastic cerebellar degeneration – an autoimmunedisease characterized by neurodegeneration in the cerebellum. Paraneoplastic syndromes are believed to be triggered by ectopic tumour expression of neuronal proteins. The CDR1 protein is expressed by neurons in the cerebellar cortex and in certain cancers. In this study, we characterized the subcellular localization of CDR1 to help delineate potential functions in cancer cells and neurons.

Methods: Ovarian cancer cells, cerebellar sections, and Purkinje cells in culture were immunostained and imaged by super-resolution stimulated emission depletion microscopy and potential interaction partners were investigated using a proximity ligation assay.

Results: CDR1 was localized to the mitochondria in cancer cells and was colocalized with proteins of the outer mitochondrial membrane. Using a proximity ligation assay, we discovered that CDR1 interacts with mitofusin 1 – a transmembrane GTPase involved in mitochondrial fusion – in both cancer cells and rat cerebellum. CDR1 also colocalized with intermediate filaments, including vimentin, in cancer cells and with neurofilaments in human cerebellum.

Conclusion: The dual localization to mitochondria and intermediate filaments as well as colocalization with key proteins involved in mitochondrial dynamics suggest that CDR1 is involved in the subcellular distribution of mitochondria in cells.

Background

Paraneoplastic cerebellar degeneration (PCD) is a rare, cancer-associated, autoimmune and neurodegenerative disease characterized by severe cerebellar dysfunction (1). PCD is closely associated with breast and ovarian cancer and occurs as an autoimmune response elicited by ectopic expression of neural antigens by the cancer cells (2). Onconeural antibodies and cytotoxic T cells target both the cancer cells and the neurons that endogenously express these antigens, ultimately causing degeneration of neurons in the cerebellar cortex (1, 3). Anti-Yo is the predominant onconeural antibody found in the serum and cerebrospinal fluid of patients with PCD (4, 5). Three cerebellar antigens have been described for anti-Yo: the cerebellar degeneration-related (CDR) proteins CDR1, CDR2, and CDR2-like (6–8). We recently demonstrated that CDR2-like, a CDR2 homolog with approximately 50% sequence identity, is the major target of the Yo antibody in samples from patients with PCD (9).

The association between CDR1 and PCD is poorly characterized as CDR1-specific antibodies have only been reported in two patients with PCD (6, 10). CDR1 is mainly expressed in the brain including the cerebellum, cerebral cortex, basal ganglia, and the pituitary gland (11). High levels of CDR1 expression are observed in Purkinje cells and the interneurons of the cerebellar cortex (6, 10). Transcriptomic profiling showed higher *CDR1* expression in ovarian tumours from PCD patients than in ovarian tumours from patients without PCD (12). We have shown that CDR1 is also expressed in breast and ovarian tumours in

patients without PCD, but not in the corresponding healthy tissue (10). Overexpression of CDR1 has been reported in prostate cancer cell lines (13), suggesting that CDR1 is involved in several types of cancers.

In glioblastoma cells, Li et al. (14) found that overexpression of CDR1 is associated with reduced proliferation, migration, and invasion and increased apoptosis. However, the expression of CDR1 in glioblastoma is downregulated compared to levels in normal brain tissue, likely due to negative regulation by the microRNA miR-671-5p (14). The expression of CDR1 is positively regulated by the *CDR1* antisense strand (*CDR1as*, also known as ciRS-7), which is a non-coding, circular RNA that acts as a microRNA sponge. *CDR1as* plays an important role in post-transcriptional regulation of protein expression in the brain (15, 16). Higher than normal levels of *CDR1as* have been reported in several cancers including colorectal (17), gastric (18), and liver (19). *CDR1* mRNA is present at increased levels in patients with Alzheimer's disease (20) and prion disease (21), and decreased levels of *CDR1* mRNA are observed in patients with Huntington's disease (22).

Little is known about the distribution and function of CDR1 in the cerebellum or about its function in cancer progression. We have previously shown that CDR1 localizes to the cytosol and dendrites of Purkinje cells and to the cytosol and actin-rich protrusions of cultured cancer cells (10). Here we further characterized CDR1 by studying its subcellular localization in cancer cells, cultured Purkinje cells, and cerebellar sections.

Methods

Cell culturing

The human ovarian cancer cell line COV318 was obtained from the European Collection of Authenticated Cell Cultures. Cells were cultured in DMEM supplemented with 10% FBS, 1% L-glutamine and 1% penicillin/streptomycin in a humidified atmosphere with 5% CO_2 at 37 °C. All reagents were acquired from Thermo Fisher.

Rat Purkinje cell culture

All procedures were performed according to the National Institutes of Health Guidelines for the Care and Use of Laboratory Animals Norway (FOTS #20135149/20157494/20170001). Embryonic day 18 Wistar Hannover GLAST pups were used for neuronal culture preparation. The protocol has recently been described (23).

Cerebellar tissue

Cerebellar sections (10 µm) were cut from fresh frozen normal human tissue (REK, #2013/1503) or paraformaldehyde-perfused rat brains (The Norwegian regulation of the use of animals in research, #20157494). The rat sections required heat-induced epitope retrieval using a pressure cooker and Diva Decloaker buffer solution (Biocare Medical) prior to immunostaining.

Immunostaining and antibodies

COV318 cells and rat Purkinje cells cultured on #1.5 poly-D-lysine coated glass coverslips (Neuvitro) were fixed in 4% paraformaldehyde in phosphate-buffered saline (PBS) for 15–30 min at room temperature and demembranated with 0.2% Triton X-100 in PBS for 7 min at room temperature. A 5 min incubation in 50 mM NH_4Cl in PBS quenched autofluorescence of the samples. Blocking was performed with 33% Sea Block blocking buffer (Thermo Fisher) in PBS for 1 h at room temperature. Primary and secondary antibodies were diluted in PBS with 10% Sea Block. Incubations with primary antibodies were performed over night at 4 °C, and secondary antibodies were incubated for 1 h at room temperature. Three 20 min washes in PBS were performed following incubation with primary and secondary antibodies. The coverslips were mounted using Prolong Diamond antifade with DAPI (Thermo Fisher). Immunostaining of the cerebellar sections was performed in the same way with the exceptions that the blocking solution and the antibody diluent also containing 1% and 0.33% Triton X-100, respectively.

Antibodies against CDR1 were made by Eurogentec by immunizing a rabbit with a CDR1 peptide sequence (amino acids 99–129). Rabbit anti-CDR1 was used at dilutions of 1:250 for immunofluorescence and 1:1000 for western blot. Antibodies used for immunofluorescence and proximity ligation assay were as follows: mouse anti-GRP75 (Abcam #ab2799), mouse anti-TUFM (Merck #AMAB90966), mouse anti-SDHB (Abcam #ab14714), mouse anti-TOMM20 (Abcam #ab56783), mouse anti-mitofusin1 (Abcam #ab57602), mouse anti-Miro2 (Abcam #ab67588), mouse anti-ß-tubulin (Merck #T4026), mouse anti-ß-actin (Abcam #ab6276), phalloidin STAR 635 conjugate (Merck #30972), mouse anti-vimentin (Abcam #ab8978), mouse anti-cytokeratin 8 (Abcam #ab9023), mouse anti-neurofilament light (Abcam #7255), chicken anti-neurofilament heavy (Abcam #ab4680), mouse anti-GFAP (BD Biosciences #561470), and guinea pig anti-calbindin D28k (Synaptic Systems #214005). All primary antibodies were diluted 1:250 with the exception of the antibodies to cytoskeletal markers and calbindin D28k, which were diluted 1:500.

Species-specific fluorescent secondary antibodies were as follows: goat anti-chicken Alexa Fluor 488 (Thermo Fisher #A-11039), goat anti-guinea pig Alexa Fluor 488 (Thermo Fisher # A-11073), goat anti-rabbit STAR 580 (Abberior #ST580), and goat anti-mouse STAR 635P (Abberior #ST635P).

Fluorescence microscopy and STED imaging

Confocal and STED images were acquired with a commercial Leica TCS SP8 STED 3X microscope equipped with an inverted DMi8 microscope and a 100x, NA 1.4 oil immersion objective (HC PL APO CS2; Leica Microsystems). Optimal excitation wavelengths were selected from a 1.5 mW pulsed white-light laser with a tuneable range of 470–670 nm. Stimulated emission depletion (STED) was performed with a 1.5 W, pulsed, 775 nm STED laser with the depletion power set to 675 mW. All images were acquired in 2D STED mode. Fluorescence signals were passed through a 0.93-1.0 Airy unit pinhole and detected with Leica HyD hybrid photodetectors with a gain of 100% and a time gate of $0.5 \leq$ time gate ≤ 7 ns. Imaging and setup of scans was done using standard Leica Application Suite X (LAS X) software. All images were acquired sequentially between frames to minimize spectral bleed-through. Photobleaching during image acquisition was negligible. All images were collected as a z-stack of several focal planes.

Proximity ligation assay

Proximity ligation assay (PLA) was carried out using the Duolink PLA in situ kit (Merck). Only target proteins in close proximity (< 40 nm) generate fluorescent signals indicating a successful PLA reaction. PLA was performed according to the manufacturer's instructions with the exception that blocking and dilution of primary antibodies were performed with Sea Block in a step similar to that performed for immunostaining. For PLA, the COV318 cells were fixed as described above on 8-well glass slides (Ibidi). Samples were incubated with a combination of anti-CDR1 and primary antibodies against mitochondrial and cytoskeletal proteins over night at 4 ˚C. This was followed by incubation with species-specific secondary antibodies conjugated to PLA MINUS and PLUS probes. The samples were mounted using Prolong Diamond antifade with DAPI. Imaging was performed with the Leica TCS SP8 STED 3X microscope.

Subcellular fractionation

Isolation of mitochondria from COV318 cells was performed with a mitochondria isolation kit (MACS Miltenyi Biotec) according to the manufacturer's instructions. This protocol utilizes magnetically labelled beads to extract intact mitochondria from whole cell lysates. Fractions were analysed using SDS-PAGE and immunoblotting.

Western blot analysis

COV318 cells were lysed in radio-immunoprecipitation assay lysis buffer (G-Biosciences; 25 mM Tris, 150 mM NaCl, 1% NP-40, 1% sodium deoxycholate, 0.1% SDS, pH 7.6) supplemented with protease (Halt Protease Inhibitor Cocktail; Thermo Fisher) and phosphatase inhibitors (PhosSTOP; Merck). Protein concentration was determined using Pierce BCA protein assay kit (Thermo Fisher). Rat cerebellar lysates were prepared by homogenization of normal adult rat cerebellum followed by lysis using a total protein extraction kit (Millipore). Human cerebellar lysate was purchased from ProSci. Proteins were separated on precast 12% SDS-PAGE gels and transferred to PVDF membranes using the Trans Blot Turbo Transfer Pack on the Trans-Blot Turbo system. Membranes were blocked with 5% non-fat dry milk in PBS with 0.05% Tween for 1 h at room temperature. Primary and secondary antibodies were diluted in PBS with 0.05% Tween and 0.5% dry milk. Membranes were incubated with rabbit anti-CDR1 (1:1000) over night at 4 °C followed by incubation with swine anti-rabbit HRP antibody (1:2000; DAKO) for 1 h at room temperature. The blots were developed using chemiluminescence with Clarity Western ECL substrates and imaged on ChemiDoc XRS+. All western blots were repeated at least three times with reproducible results. All materials, reagents and equipment were acquired from Bio Rad.

Results

CDR1 colocalizes with mitochondria and cytoskeletal filaments in cancer cells

CDR1 is expressed in ovarian tumours (10), so to evaluate the subcellular localization of CDR1, we used an ovarian cancer cell line. Immunofluorescence imaging revealed two distinct structures stained for CDR1 in addition to diffuse cytoplasmic and nuclear staining. Most prominent was the network of tubules extending from the nuclei and outwards into the cytoplasm. Co-staining for several mitochondria-specific proteins revealed that these were mitochondrial tubules (Fig. 1A). Using super-resolution STED microscopy, we found that the CDR1 staining formed a punctate pattern along mitochondrial tubules. The use of proximity ligation assay (PLA) further supported the localization of CDR1 to mitochondria (Fig. 1B). Mitochondria were stained with a selection of antibodies against mitochondrial proteins residing in the matrix (HSP60, TUFM), the inner membrane (SDHB), or the outer membrane (TOMM20, mitofusin 1, Miro2). Using PLA, we found that CDR1 interacts with mitofusin 1, Miro2 and TOMM20, proteins that reside in the outer mitochondrial membrane.

In a subset of the cancer cells, the antibody to CDR1 also stained filamentous structures that had a heterogenous appearance. Some formed thick filaments that encircled the nuclei and extended toward the cell periphery, some formed junctions between adjacent cells, and others formed more delicate networks in the cytoplasm. Co-staining with markers for all major components of the cytoskeleton showed that the majority of these structures colocalized with intermediate filaments, particularly vimentin (Fig. 1C). Vimentin and cytokeratin 8 were not expressed in all cells (Fig. 1C). This was supported by PLA: Fluorescent signals between CDR1 and the intermediate filaments were only observed in some of the cells (Fig. 1D, images 3–4). Some colocalization with actin filaments was seen at the periphery of some cells, and only limited interactions between CDR1 and microtubules were observed (Fig. 1D, images 1–2).

CDR1 colocalizes with mitofusin 1 and neurofilaments in the cerebellum

Since CDR1 is normally expressed in the cerebellum (6, 10), we also studied whether CDR1 colocalizes with mitochondria and intermediate filaments in cerebellum as it does in cancer cells. In rat cerebellum, CDR1 antibodies stained the cortex, particularly the large Purkinje cells (Fig. 2, image 1). Co-staining for calbindin, a Purkinje cell marker, confirmed that CDR1 was present in both the soma and dendrites of Purkinje cells. Due to more diffuse CDR1 staining in the Purkinje cell soma compared to the cancer cells, no tubular mitochondria staining was observed. However, there was overlap of staining for mitofusin 1 and CDR1 in both the Purkinje cells and in the surrounding tissue (Fig. 2, images 2–4), which was confirmed by PLA (data not shown). No colocalization was seen for mitofusin 2 (data not shown).

In human cerebellum, CDR1 antibodies stained the Purkinje cells and dendrites. In the Purkinje cell soma, a punctate pattern of CDR1 staining surrounding the nucleus was observed (Fig. 2, image 8). We were not able to identify these structures, as no clear colocalization was seen with any of the tested organelle markers (data not shown; supplementary table 1). CDR1 also stained neurofilaments surrounding the Purkinje cell soma and in the adjacent granular layer (Fig. 2, images 5–8), which was confirmed by PLA (data not shown). Some colocalization was also observed with the intermediate filament protein GFAP.

CDR1 colocalizes with mitofusin 1 and neurofilaments in Purkinje cells in culture

To further elucidate the localization of CDR1 in Purkinje cells, we used a dissociated rat Purkinje cell primary culture. Immunofluorescence imaging of CDR1 in the cultures showed only weak staining of the Purkinje cells; however, CDR1 antibodies strongly stained the axons from the other neurons found throughout the culture and colocalized with neurofilaments (Fig. 3, images 1–4). Some overlap was also seen with GFAP (data not shown). Similar to the rat cerebellar sections, CDR1 also colocalized with mitofusin 1, which was present in the axons (Fig. 3, images 5–7); this colocalization was confirmed by PLA (Fig. 3, image 8).

Expression of CDR1 in cancer cells and cerebellar tissue

Lysates from ovarian cancer cells and cerebellar tissue were analysed for CDR1 using SDS-PAGE and western blotting. The cancer cells had two distinct bands, a strong band at approximately 37 kDa and a weaker band at approximately 40 kDa (Fig. 4A). The rat and human cerebellum similarly had strong bands at 37 kDa, as well as weak bands at around 40 kDa. We performed subcellular fractionation of the cancer cells and found that only the 40 kDa band was present in the mitochondrial fraction (Fig. 4B).

Discussion

CDR1 is associated with the paraneoplastic neurodegenerative disease PCD, and increased levels of CDR1 expression are observed in ovarian cancer (10). However, the functional properties of the protein in the brain and in cancer are unknown. Using a combination of cancer cells and brain tissue, we have investigated the subcellular localization of CDR1 and its potential interaction partners. In ovarian cancer cells, we found that the majority of CDR1 is localized to mitochondria with a clustered distribution along mitochondrial tubules. Using PLA, we found that CDR1 is closely associated with the outer mitochondrial membrane. CDR1 colocalized with mitofusin 1 – a transmembrane GTPase that mediates mitochondrial fusion (24). This colocalization was seen in cancer cells in culture, the rat cerebellum, and the Purkinje cell culture. In the human cerebellum however only partial colocalization was seen. In human cerebellum, anti-CDR1 antibodies stained small clusters in the Purkinje cell soma but did not colocalize with any of the mitochondrial proteins or organelle markers tested.

According to the MitoMiner database of mitochondrial localization data (25), CDR1 is not predicted to have a mitochondrial targeting sequence at its N-terminus. However, some proteins interact with the outer mitochondrial membrane in a dynamic manner. Post-translational modifications can regulate this interaction. The CDR1 protein has at least three high probability sites for O-linked glycosylation (26). Furthermore, we found that CDR1 antibodies identify two distinct bands on western blot, and only the higher molecular weight band was present in the mitochondrial fraction. It is therefore possible that post-translational modifications like glycosylation contribute to the association of CDR1 with mitochondria. Several mitochondria-associated proteins have been found to have glycosylated isoforms (27). For

example, O-linked glycosylation modulates the recruitment of the mitochondrial fission protein Drp1 (28) and regulates mitochondrial transport in neurons through glycosylation of the adaptor protein TRAK (also known as Milton) (29).

We also found that CDR1 is localized to filamentous structures, but these were only prominent in a subset of the cancer cells. A majority of these structures consisted of the intermediate filament protein vimentin. Some colocalization was also seen with cytokeratin 8, and it is likely that other cytokeratins would yield similar results. Only some of the ovarian cells in the culture expressed vimentin and cytokeratin 8 and showed overlapping CDR1 staining. This differential expression of the intermediate filaments may explain why only some of the cells had filamentous structures stained by CDR1. Vimentin expression is a marker for the epithelial-to-mesenchymal transition (EMT), a process by which cells alter their gene expression programme resulting in increased motility and invasive capabilities (29). The EMT also affects mitochondrial dynamics. Wu et al. (30) found that EMT induces mitochondrial fusion through upregulation of mitofusin 1. As we found that CDR1 colocalizes with mitofusin 1, it is possible that the expression of CDR1 is affected by the EMT in cancer cells.

Colocalization between CDR1 and intermediate filaments was also observed in the Purkinje cell cultures and in human cerebellar sections. There was little vimentin staining in Purkinje cells, instead CDR1 colocalized with neurofilaments and to a lesser extent with GFAP. GFAP is expressed in astrocytes and certain other glial cells, whereas neurofilaments provide structural support for neurons, especially for radial growth of myelinated axons. In contrast to our observation in cerebellar sections, CDR1 antibodies showed only weak staining of the Purkinje cells in culture. This is probably due to the different age of the Purkinje cells in culture (harvested on embryonic day 18; matured for three weeks) and cerebellar sections (harvested from adults). CDR1 may therefore be expressed age-dependently in the Purkinje cells, which is the case for other Purkinje-related proteins (30).

The dual localization of CDR1 on mitochondria and on cytoskeletal filaments suggests that it functions in both structures. Mitochondria depend on interactions with the cytoskeleton to accumulate at regions with high energy demands, such as the leading edge of cancer cells during cell migration and matrix invasion (31) and axonal domains like growth cones and presynaptic terminals (32, 33). Long-range mitochondrial transport is primarily mediated by microtubules, whereas actin filaments mediate shorter range movements and anchoring, important in growth cones and dendritic spines (34, 35). The outer mitochondrial membrane GTPase Miro and the motor adaptor TRAK are key mediators of mitochondrial transportation through coupling of mitochondria to motor proteins (34). We used PLA to investigate the association between CDR1 and this transport machinery in the cancer cells and found that CDR1 colocalized with Miro2, which is critical for actin-dependent transport (34). We also observed CDR1 within actin-rich structures at the periphery of the cancer cells. To ensure proper distribution of mitochondria, there is extensive crosstalk between the transportation and fusion-fission machinery, and the Miro proteins have been found to interact with the mitofusin proteins (34, 36). Since we found that CDR1 is colocalized with mitofusin 1, it is therefore likely that CDR1 is part of a protein complex important for mitochondrial dynamics.

Due to their apolarity, intermediate filaments cannot provide directional cues for mitochondrial transport (37). Instead, intermediate filaments like vimentin and neurofilaments anchor the mitochondria within the cytoplasm (38, 39), and this affects mitochondrial morphology, motility, and distribution (38–41). Intermediate filaments bind to mitochondria via intermediate filament-associated proteins. As we found CDR1 both at the outer mitochondrial membrane and on vimentin and neurofilaments, we hypothesise that CDR1 is involved in the interaction between mitochondria and intermediate filaments. A similar function has been shown for the cytolinker protein plectin 1b, which tethers mitochondria to intermediate filaments and thereby affects the shape and formation of the mitochondrial network (42). Like CDR1, plectin 1b colocalizes with both mitochondria and vimentin (42). Furthermore, plectin 1b was found to be associated with the mitochondrial fusion machinery, as plectin 1b deficiency caused an upregulation of mitofusin 2 (43). Taken together, the colocalization of CDR1 with key proteins involved in mitochondrial transport and fusion and with intermediate filaments suggests that CDR1 is involved in the subcellular distribution of mitochondria in cells. As highly energy-demanding cells, cancer cells and neurons may therefore benefit from upregulating the expression of CDR1.

Disruption of normal mitochondrial function is a common pathological feature of neurodegenerative diseases. Deficiency of key regulators of mitochondrial transport and fusion-fission impairs mitochondrial distribution, causing depletion of mitochondria from dendrites and axons and subsequent loss of dendritic spines and synapses (44–46). For example, neurons with reduced expression of the mitofusin proteins have dysfunctional mitochondria and altered Ca^{2+} homeostasis, which leads to increased excitotoxicity and neuronal death (47). Levels of expression of mitofusin 1 are decreased in patients with Alzheimer's disease (48), amyotrophic lateral sclerosis (49), and Huntington's disease (50). Our findings linking CDR1 with mitofusin 1 suggest that CDR1 may be affected by or may contribute to the mitochondrial dysfunction in neurodegeneration. Interestingly, expression of CDR1 is also dysregulated in Alzheimer's disease (20), Huntington's disease (22), and prion disease (21), and mitochondrial dysfunction is also likely to contribute to the pathogenesis of PCD (51).

Conclusions

In conclusion, we found that CDR1 is mainly localized to mitochondria in cancer cells, with accumulation at the outer mitochondrial membrane. CDR1 was also localized to cytoskeletal filaments, particularly intermediate filaments. Similar results were found in cerebellar tissue where CDR1 colocalized with mitofusin 1 and neurofilaments. The dual localization to mitochondria and cytoskeletal filaments, as well as colocalization with key proteins involved in mitochondrial dynamics suggest that CDR1 is involved in subcellular distribution of mitochondria in cells, an essential function that is dysregulated in cancer and neurodegeneration.

List Of Abbreviations

CDR1	Cerebellar degeneration-related protein 1
CDR1as	*CDR1* antisense strand
EMT	Epithelial-to-mesenchymal transition
PBS	Phosphate-buffered saline
PCD	Paraneoplastic cerebellar degeneration
PLA	Proximity ligation assay
STED	Stimulated emission depletion

Declarations

Ethics approval and consent to participate

The use of human cerebellar tissue was approved by the Regional Committees for Medical and Health Research Ethics (REK, #2013/1503). The use of rats for preparation of Purkinje cell cultures and cerebellar sections were approved by the Norwegian Food Safety Authority (FOTS 20135149/20157494/20170001).

Consent for publication

Not applicable.

Availability of data and materials

Data sharing is not applicable to this article as no datasets were generated or analysed during the current study.

Competing interests

The authors declare that they have no competing interests.

Funding

Funding for this work was provided by grants from The Research Council of Norway, project number 288164.

Authors’ contributions

E.T.S., C.T., and C.A.V. contributed to the inception and design of the study; T.K. prepared the Purkinje neuron cultures; E.T.S and C.T. contributed to the acquisition and analysis of data; E.T.S., C.T., T.K., and C.A.V. drafted the text and prepared figures. All authors read and approved the final manuscript.

Acknowledgements

Technical assistance was provided by doctoral research fellow Ida Herdlevær and staff engineer Mette Haugen. All fluorescent imaging was performed at the Molecular Imaging Centre, Department of Biomedicine, University of Bergen, Norway. Neuro-SysMed is jointly hosted by Haukeland University Hospital and University of Bergen and supported as a Centre for Clinical Treatment Research (FKB) by grants from The Research Council of Norway, project number 288164.

References

1. Fanous I, Dillon P. Paraneoplastic neurological complications of breast cancer. Exp Hematol Oncol. 2015;5:29.
2. de Beukelaar JW, Sillevis Smitt PA. Managing paraneoplastic neurological disorders. Oncologist. 2006;11(3):292–305.
3. Darnell RB, Posner JB. Paraneoplastic syndromes involving the nervous system. N Engl J Med. 2003;349(16):1543–54.
4. Shams'ili S, Grefkens J, de Leeuw B, van den Bent M, Hooijkaas H, van der Holt B, et al. Paraneoplastic cerebellar degeneration associated with antineuronal antibodies: analysis of 50 patients. Brain. 2003;126(Pt 6):1409–18.
5. Rojas-Marcos I, Rousseau A, Keime-Guibert F, Rene R, Cartalat-Carel S, Delattre JY, et al. Spectrum of paraneoplastic neurologic disorders in women with breast and gynecologic cancer. Med (Baltim). 2003;82(3):216–23.
6. Furneaux HM, Dropcho EJ, Barbut D, Chen YT, Rosenblum MK, Old LJ, et al. Characterization of a cDNA encoding a 34-kDa Purkinje neuron protein recognized by sera from patients with paraneoplastic cerebellar degeneration. Proc Natl Acad Sci U S A. 1989;86(8):2873–7.
7. Darnell JC, Albert ML, Darnell RB. Cdr2, a target antigen of naturally occuring human tumor immunity, is widely expressed in gynecological tumors. Cancer Res. 2000;60(8):2136–9.
8. Eichler TW, Totland C, Haugen M, Qvale TH, Mazengia K, Storstein A, et al. CDR2L Antibodies: A New Player in Paraneoplastic Cerebellar Degeneration. PLoS One. 2013;8(6):e66002.
9. Krakenes T, Herdlevaer I, Raspotnig M, Haugen M, Schubert M, Vedeler CA. CDR2L Is the Major Yo Antibody Target in Paraneoplastic Cerebellar Degeneration. Ann Neurol. 2019.
10. Totland C, Kråkenes T, Mazengia K, Haugen M, Vedeler C. Expression of the onconeural protein CDR1 in cerebellum and ovarian cancer. Oncotarget. 2018;9(2):23975–86.

11. The Human Protein Atlas. https://www.proteinatlas.org/ENSG00000184258-CDR1/tissue. Accessed 25 May, 2020.
12. Vialatte de Pémille C, Berzero G, Small M, Psimaras D, Giry M, Daniau M, et al. Transcriptomic immune profiling of ovarian cancers in paraneoplastic cerebellar degeneration associated with anti-Yo antibodies. Br J Cancer. 2018;119(1):105–13.
13. Salemi M, Fraggetta F, Galia A, Pepe P, Cimino L, Condorelli RA, et al. Cerebellar degeneration-related autoantigen 1 (CDR1) gene expression in prostate cancer cell lines. Int J Biol Markers. 2014;29(3):e288-90.
14. Li X, Diao H. Circular RNA circ_0001946 acts as a competing endogenous RNA to inhibit glioblastoma progression by modulating miR-671-5p and CDR1. J Cell Physiol. 2019;234(8):13807–19.
15. Memczak S, Jens M, Elefsinioti A, Torti F, Krueger J, Rybak A, et al. Circular RNAs are a large class of animal RNAs with regulatory potency. Nature. 2013;495(7441):333–8.
16. Hansen TB, Wiklund ED, Bramsen JB, Villadsen SB, Statham AL, Clark SJ, et al. miRNA-dependent gene silencing involving Ago2-mediated cleavage of a circular antisense RNA. EMBO J. 2011;30(21):4414–22.
17. Weng W, Wei Q, Toden S, Yoshida K, Nagasaka T, Fujiwara T, et al. Circular RNA ciRS-7-A Promising Prognostic Biomarker and a Potential Therapeutic Target in Colorectal Cancer. Clin Cancer Res. 2017;23(14):3918–28.
18. Pan H, Li T, Jiang Y, Pan C, Ding Y, Huang Z, et al. Overexpression of Circular RNA ciRS-7 Abrogates the Tumor Suppressive Effect of miR-7 on Gastric Cancer via PTEN/PI3K/AKT Signaling Pathway. J Cell Biochem. 2018;119(1):440–6.
19. Yu L, Gong X, Sun L, Zhou Q, Lu B, Zhu L. The Circular RNA Cdr1as Act as an Oncogene in Hepatocellular Carcinoma through Targeting miR-7 Expression. PLoS One. 2016;11(7):e0158347.
20. Bosco P, Spada R, Caniglia S, Salluzzo MG, Salemi M. Cerebellar degeneration-related autoantigen 1 (CDR1) gene expression in Alzheimer's disease. Neurol Sci. 2014;35(10):1613–4.
21. Satoh J, Yamamura T. Gene expression profile following stable expression of the cellular prion protein. Cell Mol Neurobiol. 2004;24(6):793–814.
22. Hodges A, Strand AD, Aragaki AK, Kuhn A, Sengstag T, Hughes G, et al. Regional and cellular gene expression changes in human Huntington's disease brain. Hum Mol Genet. 2006;15(6):965–77.
23. Uggerud IM, Krakenes T, Hirai H, Vedeler CA, Schubert M. Development and optimization of a high-throughput 3D rat Purkinje neuron culture. bioRxiv. 2020:2020.05.20.105858.
24. Schrepfer E, Scorrano L. Mitofusins, from Mitochondria to Metabolism. Mol Cell. 2016;61(5):683–94.
25. Smith AC, Robinson AJ. MitoMiner, an integrated database for the storage and analysis of mitochondrial proteomics data. Mol Cell Proteomics. 2009;8(6):1324–37.
26. Steentoft C, Vakhrushev SY, Joshi HJ, Kong Y, Vester-Christensen MB, Schjoldager KT, et al. Precision mapping of the human O-GalNAc glycoproteome through SimpleCell technology. EMBO J.

2013;32(10):1478–88.
27. Burnham-Marusich AR, Berninsone PM. Multiple proteins with essential mitochondrial functions have glycosylated isoforms. Mitochondrion. 2012;12(4):423–7.
28. Gawlowski T, Suarez J, Scott B, Torres-Gonzalez M, Wang H, Schwappacher R, et al. Modulation of dynamin-related protein 1 (DRP1) function by increased O-linked-β-N-acetylglucosamine modification (O-GlcNAc) in cardiac myocytes. J Biol Chem. 2012;287(35):30024–34.
29. Pekkurnaz G, Trinidad JC, Wang X, Kong D, Schwarz TL. Glucose regulates mitochondrial motility via Milton modification by O-GlcNAc transferase. Cell. 2014;158(1):54–68.
30. Kumar A, Gibbs JR, Beilina A, Dillman A, Kumaran R, Trabzuni D, et al. Age-associated changes in gene expression in human brain and isolated neurons. Neurobiol Aging. 2013;34(4):1199–209.
31. Cunniff B, McKenzie AJ, Heintz NH, Howe AK. AMPK activity regulates trafficking of mitochondria to the leading edge during cell migration and matrix invasion. Mol Biol Cell. 2016;27(17):2662–74.
32. Smith GM, Gallo G. The role of mitochondria in axon development and regeneration. Dev Neurobiol. 2018;78(3):221–37.
33. Birsa N, Norkett R, Higgs N, Lopez-Domenech G, Kittler JT. Mitochondrial trafficking in neurons and the role of the Miro family of GTPase proteins. Biochem Soc Trans. 2013;41(6):1525–31.
34. Lopez-Domenech G, Covill-Cooke C, Ivankovic D, Halff EF, Sheehan DF, Norkett R, et al. Miro proteins coordinate microtubule- and actin-dependent mitochondrial transport and distribution. EMBO J. 2018;37(3):321–36.
35. Course MM, Wang X. Transporting mitochondria in neurons. F1000Res. 2016;5.
36. Misko A, Jiang S, Wegorzewska I, Milbrandt J, Baloh RH. Mitofusin 2 is necessary for transport of axonal mitochondria and interacts with the Miro/Milton complex. J Neurosci. 2010;30(12):4232–40.
37. Schwarz N, Leube RE. Intermediate Filaments as Organizers of Cellular Space: How They Affect Mitochondrial Structure and Function. Cells. 2016;5(3).
38. Nekrasova OE, Mendez MG, Chernoivanenko IS, Tyurin-Kuzmin PA, Kuczmarski ER, Gelfand VI, et al. Vimentin intermediate filaments modulate the motility of mitochondria. Mol Biol Cell. 2011;22(13):2282–9.
39. Gentil BJ, Minotti S, Beange M, Baloh RH, Julien JP, Durham HD. Normal role of the low-molecular-weight neurofilament protein in mitochondrial dynamics and disruption in Charcot-Marie-Tooth disease. FASEB J. 2012;26(3):1194–203.
40. Chernoivanenko IS, Matveeva EA, Gelfand VI, Goldman RD, Minin AA. Mitochondrial membrane potential is regulated by vimentin intermediate filaments. FASEB J. 2015;29(3):820–7.
41. Tang HL, Lung HL, Wu KC, Le AH, Tang HM, Fung MC. Vimentin supports mitochondrial morphology and organization. Biochem J. 2008;410(1):141–6.
42. Winter L, Abrahamsberg C, Wiche G. Plectin isoform 1b mediates mitochondrion-intermediate filament network linkage and controls organelle shape. J Cell Biol. 2008;181(6):903–11.

43. Winter L, Kuznetsov AV, Grimm M, Zeöld A, Fischer I, Wiche G. Plectin isoform P1b and P1d deficiencies differentially affect mitochondrial morphology and function in skeletal muscle. Hum Mol Genet. 2015;24(16):4530–44.
44. Nguyen TT, Oh SS, Weaver D, Lewandowska A, Maxfield D, Schuler MH, et al. Loss of Miro1-directed mitochondrial movement results in a novel murine model for neuron disease. Proc Natl Acad Sci U S A. 2014;111(35):E3631-40.
45. Gao J, Wang L, Liu J, Xie F, Su B, Wang X. Abnormalities of Mitochondrial Dynamics in Neurodegenerative Diseases. Antioxidants (Basel). 2017;6(2).
46. Wakabayashi J, Zhang Z, Wakabayashi N, Tamura Y, Fukaya M, Kensler TW, et al. The dynamin-related GTPase Drp1 is required for embryonic and brain development in mice. J Cell Biol. 2009;186(6):805–16.
47. Martorell-Riera A, Segarra-Mondejar M, Munoz JP, Ginet V, Olloquequi J, Perez-Clausell J, et al. Mfn2 downregulation in excitotoxicity causes mitochondrial dysfunction and delayed neuronal death. EMBO J. 2014;33(20):2388–407.
48. Wang X, Su B, Lee HG, Li X, Perry G, Smith MA, et al. Impaired balance of mitochondrial fission and fusion in Alzheimer's disease. J Neurosci. 2009;29(28):9090–103.
49. Russell AP, Wada S, Vergani L, Hock MB, Lamon S, Leger B, et al. Disruption of skeletal muscle mitochondrial network genes and miRNAs in amyotrophic lateral sclerosis. Neurobiol Dis. 2013;49:107–17.
50. Kim J, Moody JP, Edgerly CK, Bordiuk OL, Cormier K, Smith K, et al. Mitochondrial loss, dysfunction and altered dynamics in Huntington's disease. Hum Mol Genet. 2010;19(20):3919–35.
51. Panja D, Vedeler CA, Schubert M. Paraneoplastic cerebellar degeneration: Yo antibody alters mitochondrial calcium buffering capacity. Neuropathol Appl Neurobiol. 2018.

Figures

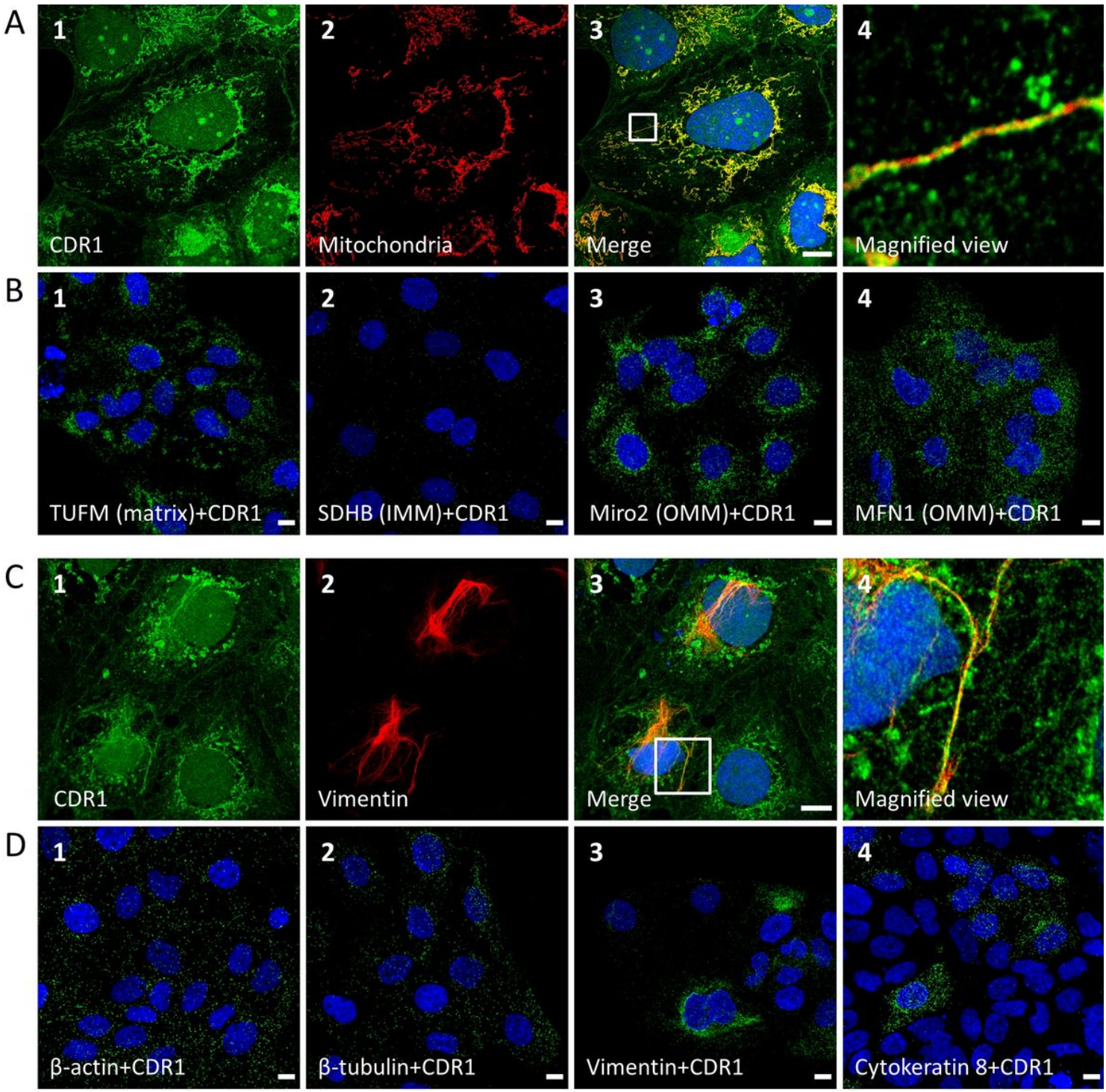

Figure 1

CDR1 colocalizes with mitochondria and intermediate filaments in ovarian cancer cells. (A) Representative images of COV318 cells stained as indicated, showing colocalization between CDR1 and mitochondria (GRP75). The panel on the far right is a 10X magnified image of the region boxed in the merged image. (B) Representative images of PLA with antibodies to CDR1 and indicated mitochondrial proteins residing in the mitochondrial matrix, the inner mitochondrial membrane (IMM), and the outer mitochondrial membrane (OMM). Each fluorescent dot indicates an interaction between the two target proteins. (C) Representative images of COV318 cells stained as indicated, showing colocalization

between CDR1 and vimentin. (D) Representative images of PLA with antibodies to CDR1 and indicated cytoskeletal proteins. Each fluorescent dot indicates an interaction between the two target proteins. Scale bars: 10 μm.

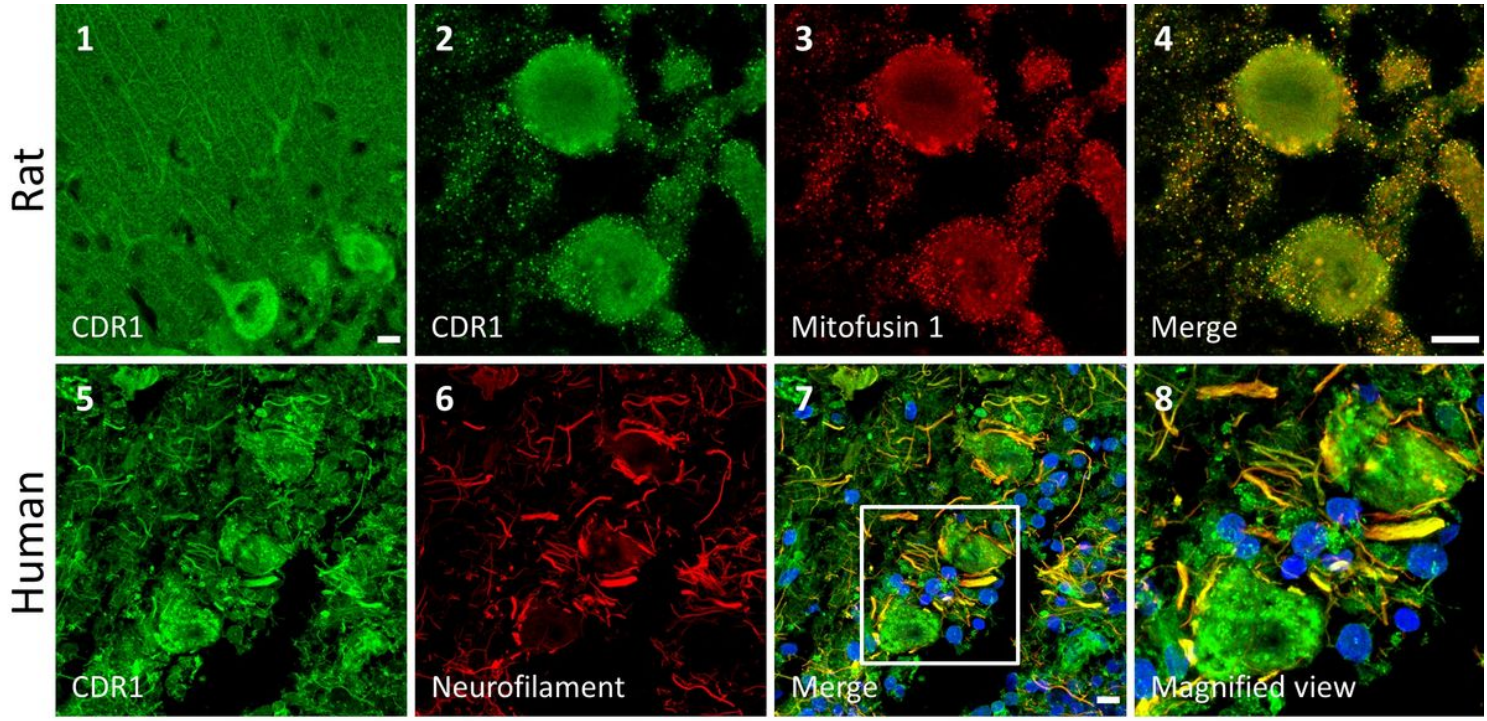

Figure 2

CDR1 staining in rat and human cerebellum. (1) Representative image of rat cerebellar cortex stained by CDR1, showing cytoplasmic and dendritic staining of the Purkinje cells. (2-4) Representative images of Purkinje cells in the rat cerebellar cortex stained as indicated, showing colocalization of CDR1 and mitofusin 1 in Purkinje cells. (5-8) Representative images of human cerebellar cortex stained as indicated, showing colocalization between CDR1 and neurofilaments.The panel on the far right is a 3X magnified image of the region boxed in the merged image. Scale bars: 10 μm.

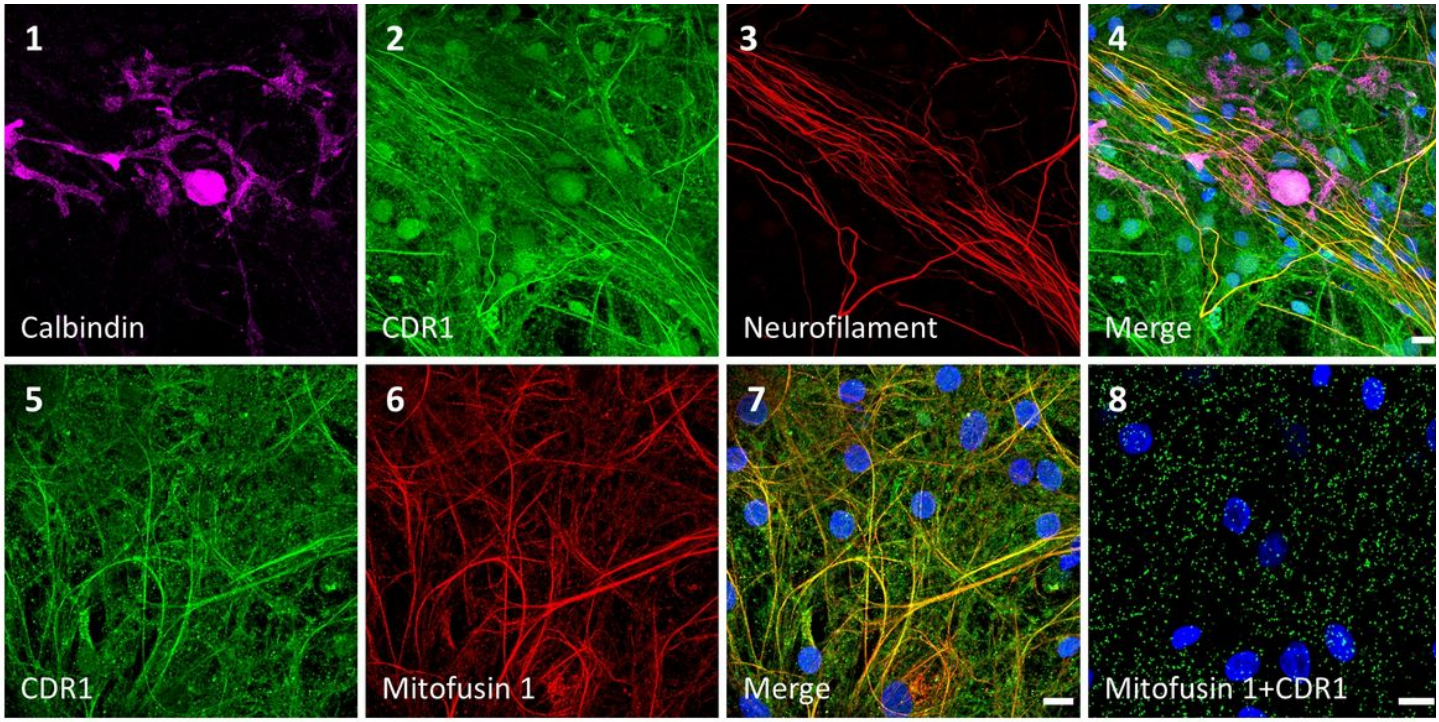

Figure 3

CDR1 staining in arat Purkinje cell culture. (1-4) Representative images of a Purkinje cell in culture stained as indicated, showing mainly colocalization between CDR1 and the surrounding neurofilaments. (5-7) Representative images of the supporting neurons in the culture stained as indicated, showing colocalization between CDR1 and mitofusin 1.Representative image of PLA with antibodies to CDR1 and mitofusin 1. Scale bars: 10 μm.

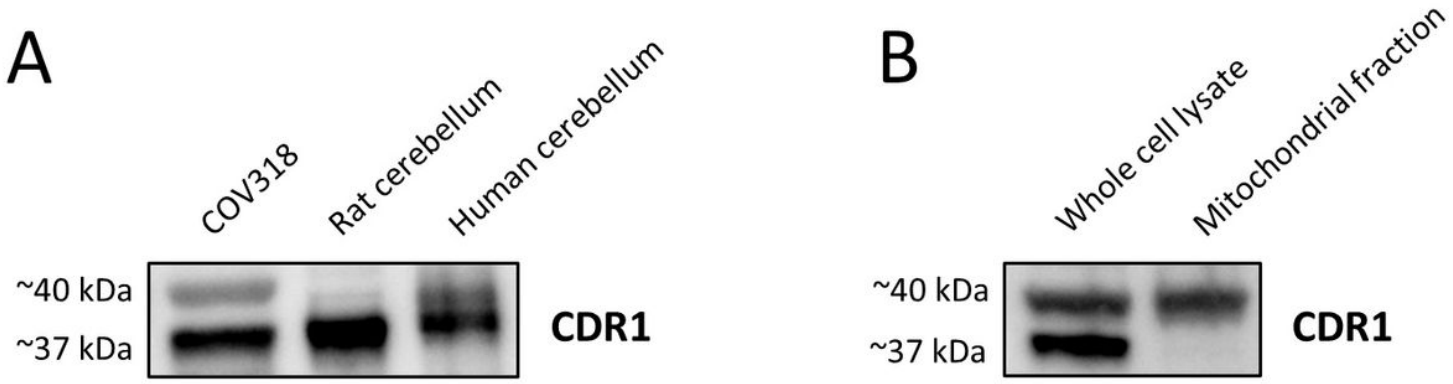

Figure 4

(A) Western blot of CDR1 expression in COV318 ovarian cancer cells (20 μg protein), rat cerebellar lysate (7.5 μg), and human cerebellar lysate (2.5 μg).Bands at approximately 37 kDa and a weaker band at approximately 40 kDa were bound by the CDR1 antibody. The 40 kDa band is a very faint doublet in the rat cerebellum. (B) Western blot of CDR1 expression in whole cell lysate and mitochondrial fraction of COV318 cells.

Supplementary Files

This is a list of supplementary files associated with this preprint. Click to download.

- SupplementaryTable1.docx